

CAN WE DECIPHER THE DYNAMICS OF THE MILKY WAY DISK FROM GAIA ?

Y. Khalil¹, B. Famaey¹, G. Monari¹ and A. Siebert¹

Abstract. The unprecedented data from the Gaia mission have revealed the complex structure of the phase-space of the Milky Way (MW) disk over a larger volume than ever before. These data should help us in the search for a complete dynamical model of the MW. We concentrate here on in-plane motions and on what they can teach us about the present-day non-axisymmetric structures of the MW Disk. In the joint presence of the central bar and spiral arms, it is particularly hard to analytically compute velocities of stars for the whole phase-space domain from a distribution function (DF) satisfying the linearized collisionless Boltzmann equation. However, the conservation of the DF in infinitesimal phase-space patches following the Hamiltonian flow allows us to compute the current DF by integrating orbits backward in time to an axisymmetric equilibrium state. In this way, we can construct a DF in the joint presence of the bar and spiral arms, and confront the models to Gaia data with observables computed with the DF. Here, we show preliminary results on the effects of the bar alone, and lay down our plans for the exploration of the space of parameters of the models to establish realistic dynamical non-axisymmetric models for the MW disk, and hopefully decipher the dynamics of the MW's spiral arms.

Keywords: Galaxy: kinematics and dynamics, Galaxy: fundamental parameters, Galaxy: structure, Galaxy: Disk, Galaxy: solar neighborhood

1 Introduction

The third data release of Gaia (DR3, Gaia Collaboration et al. 2023b) has been an important milestone in offering full 6D phase-space information for stars of the Milky Way (MW) disk over a larger volume than ever before (Gaia Collaboration et al. 2023a). Whilst stellar vertical motions have revealed in recent years a disequilibrium of the Galactic disk (Antoja et al. 2018, 2023), possibly related to a subtle interplay between external perturbations and internal non-axisymmetries (Li et al. 2023), the richness of the information contained solely within the in-plane motions of stars has not been fully exploited yet. In principle, these in-plane motions should allow us to get a precise dynamical mapping of the Galactic parameters setting the location, kinematics and dynamics of the most important non-axisymmetric structures of the MW disk namely, the bar and the spiral arms.

So far, different tracers and observations are far from converging on parameters describing the placement of each spiral arm segment in the MW disk. In particular, the observed geometry and extension of the arms may differ. The so-called Local arm, for example, has been found by Gaia Collaboration et al. (2023a) and Poggio et al. (2021), tracing young stars, to be more extended and to have an intermediary pitch angle if compared to V  zquez et al. (2008), where this arm heads outwards to the Perseus arm, or to Xu et al. (2021), where the Local arm heads inwards to the Carina-Sagittarius arm. Similar debates exist regarding the Perseus arm and Outer arm with respect to their position in the disk and pitch angle. Perhaps most strikingly, the pitch angle of the Perseus arm has been found around 24   in Levine et al. (2006), compatible with results of Poggio et al. (2021), and around 9   in Reid et al. (2019). These examples may illustrate the challenges in accurately tracing the spiral arms of the MW from photometry alone, and using the unprecedented dynamical information from Gaia could help obtaining independent constraints.

The detailed mapping of velocity space in the immediate neighbourhood of the Sun (the ‘local velocity field’, hereafter LVF) has long revealed a complex structure in the radial (v_R) vs azimuthal (v_ϕ) velocity plane where it presents a complex configuration of overdensities called moving groups (Eggen 1958; Blaauw 1970),

¹ Observatoire Astronomique de Strasbourg, Universit   de Strasbourg, UMR 7550, F-67000 Strasbourg, France

most of those being nowadays thought to be related to the orbital resonances with the bar and spiral arms of the Galaxy (Dehnen 1998, 2000; Famaey et al. 2005; Antoja et al. 2011). In particular, the so-called Hercules moving group, creating a bimodality in the local velocity distribution at low v_ϕ and positive v_R , has traditionally been associated with resonances from the Galactic bar, although some debates are still going on about which resonance to associate it to. For the other moving groups, things are even less clear, as they have been associated to various possible resonances with spiral arms (Sellwood 2010; McMillan 2011; Pompéia et al. 2011), as well as with high-order modes of the bar (Monari et al. 2019).

Regarding the mean non-axisymmetric motions of stars in a larger volume around the Sun (the ‘extended velocity field’, hereafter EVF), pioneering work has been carried out by Siebert et al. (2011) who uncovered a significant Galactocentric radial velocity gradient within a distance range limited to 2 kpc from the Sun, with data from the RAVE survey. This velocity map was explored in Siebert et al. (2012) to constrain the parameters of a Lin-Shu density wave logarithmic spiral model, notably its amplitude, pattern speed, pitch angle and number of arms. The best model found was two-armed with a location compatible with the Local and Perseus arm placements and a pattern speed of 18.6 km/s/kpc. It was noted by Monari et al. (2014) that the Galactic bar could also contribute to the gradient. With the Gaia Data Release 2 (Gaia DR2), parameters of a two-armed logarithmic spiral model were again constrained in Eilers et al. (2020): the constrained model was found to be compatible with the location of Local and Outer Arms, not giving any dynamical evidence for the Perseus arm, and with a lower pattern speed of 12 km/s/kpc. More recently, in Gaia Collaboration et al. (2023a), a full map of the average Galactocentric radial velocities of late-type RGB stars from Gaia DR3 has been produced. One can clearly identify a distinguishable signature of the Galaxy’s bar in the central regions, while other spiral-induced features seem to appear in the outskirts. It is therefore clear that a combination of the influence of the Galactic bar and spiral arms should be able to explain the main features of such a Galactocentric radial velocity map.

In the following, we describe briefly in section 2 the Gaia DR3 data subsets that we will use to confront the model at two scales: in the vicinity of the Sun (the LVF) and an extended region about 4 kpc from the Sun (the EVF). The bar model is described in 3 together with our modelling technique. In section 4 we compare the data to a bar model (without spiral arms) that already describes reasonably well the data in the LVF, similarly to the earlier results of Monari et al. (2019), but not in the EVF. We conclude in 5 on discussing the upcoming addition of spiral arms and the perspectives of this work.

2 Gaia DR3 data

From the Gaia DR3 RVS data we select stars for which we compute the positions in Galactocentric Cartesian coordinates, $\mathbf{x} = (x, y, z)$ and velocities in Galactocentric Cylindrical coordinates, $\mathbf{v} = (v_R, v_\phi, v_z)$. The coordinate transformations from original Equatorial coordinates to Galactocentric coordinates depend on the Sun’s position and velocity. For the Sun’s position, we set: $\mathbf{x}_\odot = (8.275 \text{ kpc}, 0, 15.29 \text{ pc})$, with x from GRAVITY Collaboration et al. (2021), and z from Widmark & Monari (2019). For the Sun’s velocity we use $\mathbf{v}_\odot = (9.3 \text{ kms}^{-1}, 250.2 \text{ kms}^{-1}, 7.2 \text{ kms}^{-1})$.

We select stars within $|z| < 200 \text{ pc}$, and we consider them close enough to the plane to analyze their planar motion within the $z = 0$ plane. For the LVF, we consider 909 666 stars within $r = \sqrt{(x - x_\odot)^2 + (y - y_\odot)^2} < 200 \text{ pc}$, whereas, for the EVF, we consider 12 740 039 stars within $4 \text{ kpc} < x < 12 \text{ kpc}$ and $-4 \text{ kpc} < y < 4 \text{ kpc}$. The stars of the LVF are used to study the number density distribution of stars in velocity space in the vicinity of the Sun, so we work with a 2-dimensional histogram on the (v_R, v_ϕ) -plane. The stars of the EVF are used to study the radial velocity v_R map. The data for the disk sample of Gaia DR3 data are shown in the top panels of Figure 1.

3 Model

For a joint system of bar and spiral arms with different pattern speeds there is no easy analytical description for the distribution function (DF) satisfying the linearized collisionless Boltzmann equation for the whole phase-space domain. To overcome this difficulty, we will use in our work the backwards integration method developed by Vauterin & Dejonghe (1997). Many works explored this method, notably to study the MW bar dynamics. For instance, in Dehnen (2000), the bar’s pattern speed was explored with this method and compared to the LVF obtained at the time from Hipparcos data. More recently, in Monari et al. (2019), this method was used to relate the resonances of various modes of the bar to many features of the LVF from Gaia data.

The backwards integration method is based on the conservation of the DF in infinitesimal phase-space patches following the Hamiltonian flow, which allows us to compute the current DF by integrating orbits backward in time to an axisymmetric equilibrium state, where analytical expression for the DF are well established. In this way, we can construct a DF in the joint presence of the bar and spiral arms, and confront the models to Gaia data with observables computed with the DF, mainly number density of stars in velocity space and median velocities as a function of position in the disk. We can therefore in principle explore the space of parameters of the models to establish realistic dynamical non-axisymmetric models for the MW Disk and hopefully decipher the complex non-axisymmetric structure of the disk.

In our model, we first impose a background axisymmetric potential and DF for the disk. For the time being, we then add a bar which grows smoothly. The bar potential, defined by a combination of three Fourier modes ($m = 2, 4, 6$), is described in Thomas *et al.* (2023) and inspired from the model of Portail *et al.* (2017), known to match fairly well the kinematics of the inner Galaxy. The main parameters, beyond the amplitude of the modes, are the pattern speed, Ω_{bar} and the angle of the bar's major axis in Galactocentric coordinates ϕ_b .

4 Results

Here, we set $\Omega_{\text{bar}} = 38 \text{ kms}^{-1} \text{ kpc}^{-1}$ and $\phi_b = 28^\circ$ (Monari *et al.* 2019) and display the results of this bar-only model in the bottom panels of Figure 1. Comparing the left panels of Figure 1, we confirm the results of Monari *et al.* (2019), namely that many features of the LVF can be reproduced by the bar alone. Comparing the right panels, though, it is clear that the EVF is not reproduced in the outer Galaxy. Nevertheless, it is reasonably well recovered by the bar-only model (bottom-right panel) for the region within $x < 8 \text{ kpc}$ and $y < 2 \text{ kpc}$, although some features are definitely missing even in this region.

5 Perspectives

Especially in regions beyond the Sun, the EVF obtained from our bar-only model clearly indicates the necessary inclusion of spiral arms in the model, in accordance with the precedent analysis in Siebert *et al.* (2012), and more recently in Eilers *et al.* (2020). The challenge is however to recover the EVF without destroying the already pretty satisfactory LVF. Hopefully, the inclusion of spiral arms would even improve the LVF, in regions corresponding to the Hyades and Sirius moving groups (Dehnen 1998, 2000; Famaey *et al.* 2005; Antoja *et al.* 2011; Bernet *et al.* 2022). Further development of quantitative metrics to compare model to data will allow us to explore the parameter space for spiral arms in a joint model with the bar, and more generally, to constrain parameters of the Galaxy potential, including both axisymmetric and non-axisymmetric internal structures.

References

- Antoja, T., Figueras, F., Romero-Gómez, M., *et al.* 2011, MNRAS, 418, 1423
 Antoja, T., Helmi, A., Romero-Gómez, M., *et al.* 2018, Nature, 561, 360
 Antoja, T., Ramos, P., García-Conde, B., *et al.* 2023, A&A, 673, A115
 Bernet, M., Ramos, P., Antoja, T., *et al.* 2022, A&A, 667, A116
 Blaauw, A. 1970, in *The Spiral Structure of our Galaxy*, ed. W. Becker & G. I. Kontopoulos, Vol. 38, 199
 Dehnen, W. 1998, AJ, 115, 2384
 Dehnen, W. 2000, AJ, 119, 800
 Eggen, O. J. 1958, MNRAS, 118, 65
 Eilers, A.-C., Hogg, D. W., Rix, H.-W., *et al.* 2020, ApJ, 900, 186
 Famaey, B., Jorissen, A., Luri, X., *et al.* 2005, A&A, 430, 165
 Gaia Collaboration, Drimmel, R., Romero-Gómez, M., *et al.* 2023a, A&A, 674, A37
 Gaia Collaboration, Vallenari, A., Brown, A. G. A., *et al.* 2023b, A&A, 674, A1
 GRAVITY Collaboration, Abuter, R., Amorim, A., *et al.* 2021, A&A, 647, A59
 Levine, E. S., Blitz, L., & Heiles, C. 2006, Science, 312, 1773
 Li, C., Siebert, A., Monari, G., Famaey, B., & Roziér, S. 2023, MNRAS, 524, 6331
 McMillan, P. J. 2011, MNRAS, 418, 1565
 Monari, G., Famaey, B., Siebert, A., Wegg, C., & Gerhard, O. 2019, A&A, 626, A41
 Monari, G., Helmi, A., Antoja, T., & Steinmetz, M. 2014, A&A, 569, A69

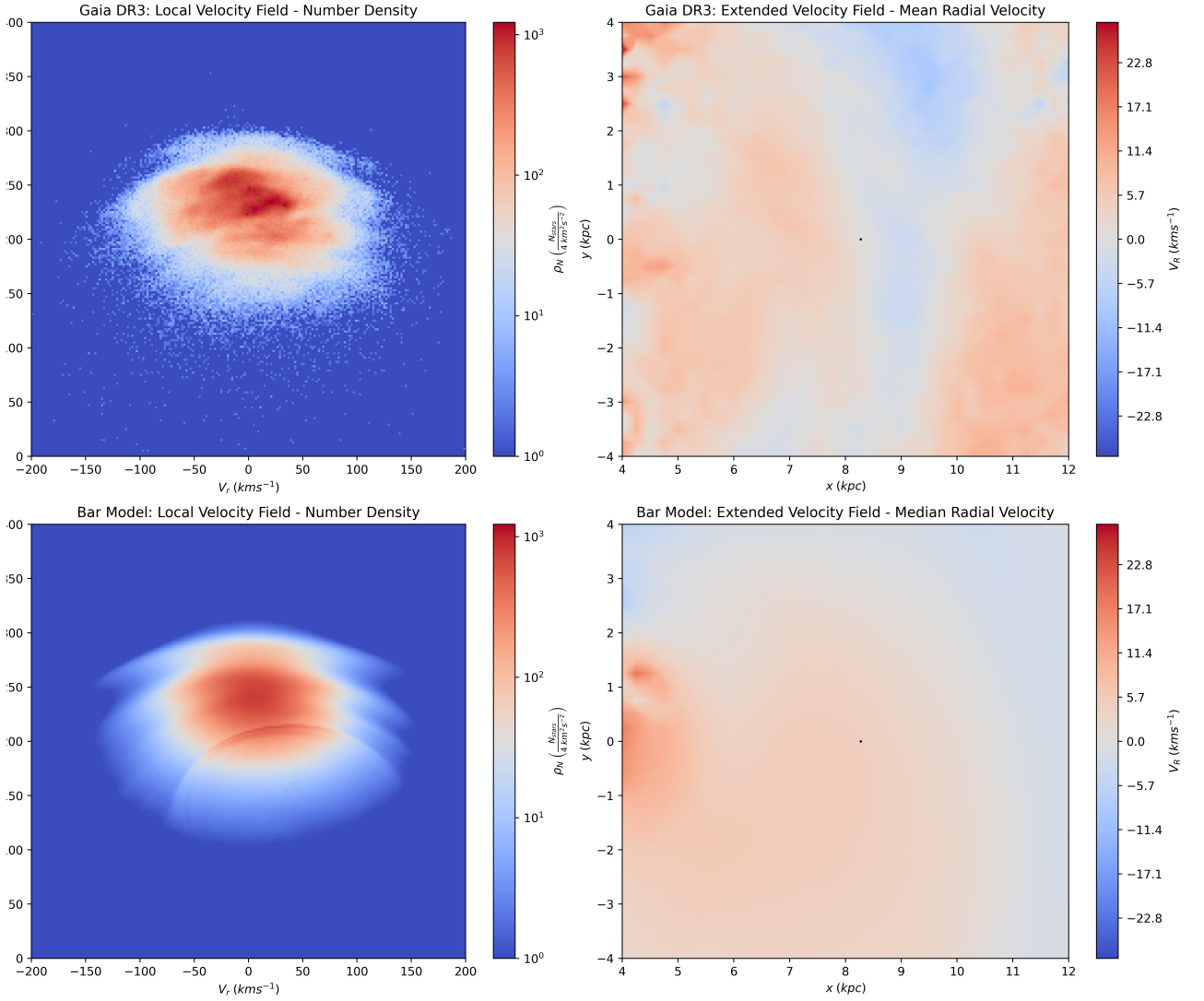


Fig. 1. Top panels: Gaia DR3 data. Bottom panels: Bar-only model. The left panels display the 2-dimensional histogram of the number density of stars for the LVF in the (v_R, v_ϕ) -plane in the Solar neighbourhood, for squared 2 kms $^{-1}$ bins. The right panels display the median Galactocentric radial velocity map for the EVF in the Galactic plane seen face-on, binned in squared 250 pc bins. The small black dot represents the Sun's position in the Galactic plane, which rotates anti-clockwise. It is clear that the bar alone reproduces many features of the LVF but not the detailed shape of the EVF, especially in the outer Galactic disk.

- Poggio, E., Drimmel, R., Cantat-Gaudin, T., et al. 2021, A&A, 651, A104
 Pompéia, L., Masseron, T., Famaey, B., et al. 2011, MNRAS, 415, 1138
 Portail, M., Gerhard, O., Wegg, C., & Ness, M. 2017, MNRAS, 465, 1621
 Reid, M. J., Menten, K. M., Brunthaler, A., et al. 2019, ApJ, 885, 131
 Sellwood, J. A. 2010, MNRAS, 409, 145
 Siebert, A., Famaey, B., Binney, J., et al. 2012, MNRAS, 425, 2335
 Siebert, A., Famaey, B., Minchev, I., et al. 2011, MNRAS, 412, 2026
 Thomas, G. F., Famaey, B., Monari, G., et al. 2023, arXiv e-prints, arXiv:2309.05733
 Vauterin, P. & Dejonghe, H. 1997, MNRAS, 286, 812
 Vázquez, R. A., May, J., Carraro, G., et al. 2008, ApJ, 672, 930
 Widmark, A. & Monari, G. 2019, MNRAS, 482, 262
 Xu, Y., Hou, L. G., Bian, S. B., et al. 2021, A&A, 645, L8